ATR of Battlefield Targets by SAR – Classification Results Using the Public MSTAR Dataset Compared with a Dataset by QinetiQ, UK

Rolf Schumacher and Kh. Rosenbach
FGAN – Forschungsgesellschaft für Angewandte Naturwissenschaften e. V.
FHR – Forschungsinstitut für Hochfrequenzphysik und Radartechnik
Neuenahrer Str. 20
D-53343 Wachtberg
GERMANY
Phone / Fax (+49) 228 9435 487 /-212

rolf.schumacher@fgan.de

SUMMARY

The development of ATR algorithms and the comparison of different classification schemes is one of the main goals of the SET-053 group. The group mainly focuses on SAR images of stationary ground targets, in which the targets are detected. These single image chips form a databank for ATR evaluation and identification to which the classification schemes can be applied. Because of the inhomogeneous measured and modelled datasets of the different nations we start our evaluation with the public MSTAR dataset, which is used since many years for ATR evaluation and identification.

In most of the publications dealing with the MSTAR dataset [1,2,3] classification rates between 97% and 100% could be reached due to the good quality of the chip images (good adjustment, centered, good signal/noise ratio, nearly exact scaling).But these results should not be overestimated because the image quality can decrease having real applications with targets in battlefield situations.

We investigate the performance of simple classification approaches when the quality of the MSTAR dataset was degraded by adding noise, decentering the targets and introducing errors in the crossrange scaling. In addition we used a dataset from real field measurements which was made available to the SET-053 group by QinetiQ,UK. As anticipated, the classification rates dropped considerable in all mentioned cases. Consequently changes in the feature extraction schemes were investigated which were able to improve the classification rates again.

Additionally we analyze the influence of clutter and target shadow on the classification rate. In both datasets the classification rate decreases when we separate the target from clutter and shadow. This is a hint, that a strict separation and segmentation of target and clutter is necessary to classify the real target. Therefore the targets should be measured independently and, if possible, at different locations, so that the clutter doesn't correlate between the test and training data. The target shadow can be used for additional information dependent on the depression angle.

By comparing different classifiers (Nearest neighbour, different types of SVMs, HNet…) we can conclude that the main work is not choosing and applying the classifier, but concentrate more on the data collection, preprocessing and feature extraction process.

Therefore in this paper the results of the different investigations concerning the preprocessing of the datasets will be presented. Main topics are the target centering, segmentation, clustering and the influence of the image resolution on the classification rate.

Paper presented at the RTO SET Symposium on "Target Identification and Recognition Using RF Systems", held in Oslo, Norway, 11-13 October 2004, and published in RTO-MP-SET-080.

1.0 INTRODUCTION

Because ATR has become more important during the last years it is essential to develop robust classification schemes, which can be applied reliably in military operations. Especially the identification of ground targets in battlefield situations is one of the most difficult tasks, because in relation to the identification of air targets [5, 6] the general conditions are much more unfavorable. The major problems are the clutter (which is not present in air), the unknown target orientation (aspect and elevation angle), high variability of the target scatterers and the possible multiple variants of the target.

2.0 DATASETS

For our investigations we use two different datasets: the public release of the MSTAR dataset and a dataset which was provided from QinetiQ (UK) to the NATO-SET-053 group. Both datasets consist of single target SAR image chips and are divided into test and training data. The following section gives a more detailed description of both databases.

2.1 MSTAR ("Public release")

The Moving and Stationary Target Acquisition and Recognition (MSTAR) was a joint Defense Advanced Research Projects Agency (DARPA) and Air Force Research Laboratory (AFRL) effort to develop and evaluate anadvanced ATR system. The program began in June of 1995 and ended in 1999. The public release of the MSTAR dataset provides approx. 20.000 SAR image chips covering 10 target types from the former Soviet Union. MSTAR has conducted three data collections in September 95, November '96 and May '97. The target images were collected near Huntsville, Alabama by the Sandia National Laboratory (SNL) using the STARLOS sensor. The imagery used here was collected as part of the MSTAR data collection #1, Scene 1 and as part of the Data Collection #2, Scenes 1,2 and 3. The targets contain three T72 Main Battle Tanks (MBT) three BMP2 Armoured Personnel Carriers (APC), a BTR70, 2S1, BDRM2, D7, T62, ZIL131, ZSU23/4 (see table 3).

The data consist of X-band SAR images with 1 foot by 1 foot resolution measured in spotlight mode. The targets have been measured over the full 360° azimuth angles with 1°-5° increments and over multiple depression angles (15°, 17°, 30° and 45°). The target data is presented as subimage chips centered on the target with a standard chip size per target type, usually 128px x 128px. Table 1 gives an overview of the dataset used in our experiments. Data collected at 15° depression angle were used for testing (3423 images) and 17° for training (3451 images).

2.2 QinetiQ SAR data

The imagery, which was kindly provided from QinetiQ (UK) to the NATO-SET-053 group, was collected from a measurement campaign in November 2001. The fully polarimetric X-band data of nine targets was recorded with the Enhanced Surveillance Radar (ESR) from QinetiQ in spotlight mode. The resolution of the images is 0.4m x 0.4m, the pixel spacing 0.3m x 0.3m, respectively. Two different circles around the target area were flown to collect training and test data separately and independently. The low depression angle of 6° caused long shadows in the images in range direction behind the targets. The squinted processing allows obtaining 360° coverage in the azimuth direction for the image dataset. Table 1 and 2 show the aspect coverage of all targets in the test and training data. Here the number of measured images is shown for an aspect interval of 10° (Asp. 1 means the interval from 0 to 9°, Asp. 2 stands for the aspect interval 10-19° and so on). The underlying colour is a measure for data density (black: no data, red: some data and white: data every 1°). We see that the training data was measured nearly completely over the whole azimuth, but the test dataset shows some gaps in the aspect angle distribution because it was measured only in some segments of the flown circle. The total ratio of train and test data is nearly 3 to 1 (330:110 for each class). In our studies we used only the HH-channel representative.

Table 1: number of images separated in 10° aspect interval (Asp. Int.) for QinetiQ training data (black: no data, red: some data, white: 1° data); Cl=target class

Asp Int. / Cl	1	2	3	4	5	6	7	8	9	10	11	12	13	14	15	16	17	18	19	20	21	22	23	24	25	26	27	28	29	30	31	32	33	34	35	36
1	9	10	10	10	9	3	10	10	10	10	10	10	10	10	10	10	10	10	10	10	10	8	5	10	10	10	10	10	10	10	10	8	2	10	10	10
2	9	10	3	10	10	10	10	10	10	10	10	10	3	7	10	10	10	10	10	10	10	4	8	10	10	10	10	10	10	10	10	10	10	10	10	10
3	1	10	10	10	10	10	10	10	10	2	10	10	10	10	10	10	10	10	10	10	10	10	10	10	10	9	4	10	10	10	10	10	10	10	10	9
4	9	10	10	10	10	8	2	10	10	10	10	10	10	10	9	3	10	10	10	10	10	10	10	10	10	10	10	10	10	10	10	8	5	10	10	10
5	9	10	10	10	10	10	10	10	10	10	10	10	8	5	10	10	10	10	10	10	10	10	8	2	10	10	10	10	10	10	10	9	3	10	10	10
6	9	10	10	10	10	10	10	10		10	10	10	10	10	10	10	10	2	10	10	10	10	10	10	10	10	10	10	10	10	10	10	10	10	3	10
7	3	9	10	10	10	10	10	10	10	4	6	10	10	10	10	10	10	10	10	5	7	10	10	10	10	10	10	10	10	10	10	10	10	10	10	10
8	4	10	10	10	10	10	10	10	9	1	10	10	10	10	10	10	10	10	10	2	10	10	10	10	10	10	10	10	10	10	10	10	10	10	10	9
9	9	10	10	10	10	10	10	10	10	10	10	6	7	10	10	10	10	10	10	10	10	6	4	10	10	10	10	10	10	10	7	5	10	10	10	10

Table 2: number of images separated in 10° aspect interval for QinetiQ test data

Asp Int. / Cl	1	2	3	4	5	6	7	8	9	10	11	12	13	14	15	16	17	18	19	20	21	22	23	24	25	26	27	28	29	30	31	32	33	34	35	36
1			1	10	5		6	10	10		3	10	8		4	5										10	6							5	10	7
2						5	10	1							10	10	2			6	10		1	10	10	5			8	10	3		9			
3		4	10	8			10	6		5	10	10	1		2	10	9		3	6										9	7					
4	5						5	10	7				1	10	5		6	10	10			3	10	8		4	5									10
5			3	10	8		4	5									10	6							5	10	7			1	10	5		6	10	10
6		8	8							3	10	9				9	7		4	10	10	2		1	10	10		2	7							
7				4	10	2							9	10	3			5	10	1		10	10	6			7	10	4		8	1				
8				9	7							4	10	8				10	6		5	10	10	1		2	10	9		3	6					
9		5	10	6		6	3								2	10	4							7	10	5			3	10	3		8	10	8	

2.3 Comparison of the MSTAR and QinetiQ dataset

Comparing the 10-class-MSTAR with the 9-class-QinetiQ dataset (Fig. 1 and 2, Table 3), the total number of images in the MSTAR train and test case are nearly the same (3671 training and 3203 test images). Each target class has approximately 300 training and 200-280 test images, which are distributed over the complete 360 azimuth homogenously. Only class 1 (BMP2) and 3 (T72) consist of trice more images because here three different serials are integrated. The training QinetiQ dataset (table 1) consists of slightly more images (330 images with nearly 1° aspect increment), but in contrast to MSTAR the test dataset (tab.2) comprises only one third of the training data (110 images per class). The aspect angle distribution of this test data is very inhomogeneous compared to the training data.

As an example for the quality of the images we see in fig. 2 a sample image from the MSTAR dataset (left) and one from the QinetiQ dataset (right). The differences between these datasets are: The MSTAR image is centered a priori and has a good signal to clutter ratio. Furthermore the clutter is distributed very homogeneously. The QinetiQ data are not centered a priori, and the S/C ratio is lower than in the MSTAR data. The target shadows in the MSTAR dataset are pronounced in contrast than the longer target shadows in the QinetiQ data.

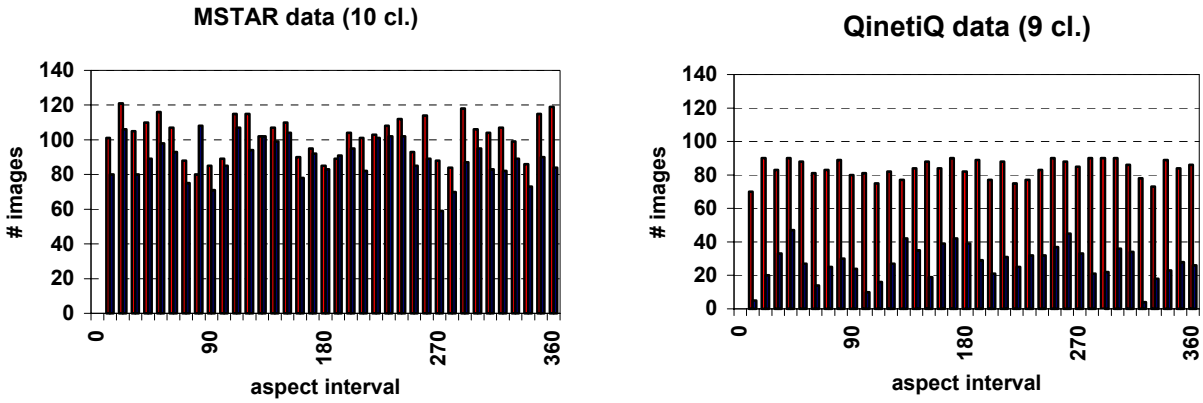

Figure 1: total number of training (red) and test (blue) images in 10° aspect interval for the MSTAR 10-class data (l.) and the 9- class QinetiQ data (r.)

Table 3: number of images per class for the MSTAR and QINETIQ dataset

	Class Type	*1 BMP2*	*2 BTR70*	*3 T72*	*4 BTR60*	*5 2S1*	*6 BRDM2*	*7 D7*	*8 T62*	*9 ZIL131*	*10 ZSU23/4*	**Sum**
MSTAR	**Train 17° dep**	698	233	691	256	299	298	299	299	299	299	3671
	Test 15° dep	587	196	582	195	274	274	274	273	274	274	3203
QinetiQ	***Class***	***1*** -	***2*** -	***3*** -	***4*** -	***5*** -	***6*** -	***7*** -	***8*** -	***9*** -		**Sum**
	Train Circ 1	330	335	335	335	335	335	335	335	335		3015
	Test Circ 2	110	110	110	110	110	111	110	110	110		991

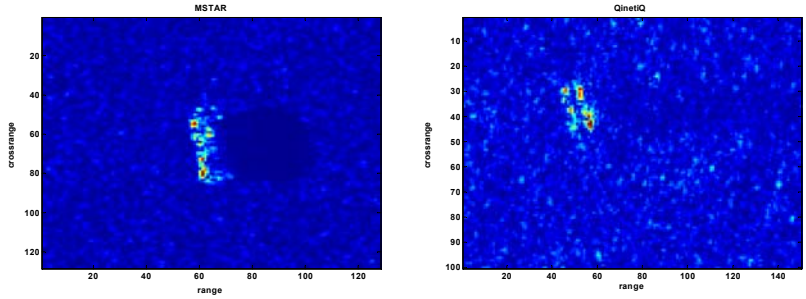

Figure 2: Sample images from datasets MSTAR (l.) and QinetiQ (r.)

3.0 DATA PREPROCESSING SCHEMES

Because we want to classify the target (and not the clutter) it is not much meaningful to take the complete original images as input for the classifier. The main work before doing classification is the preprocessing and feature extraction of the data. In order to standardize the information of each image to be classified some degree of preprocessing is required, so that the images are adjusted for the used classifier. For our further investigations we used the following processing scheme:

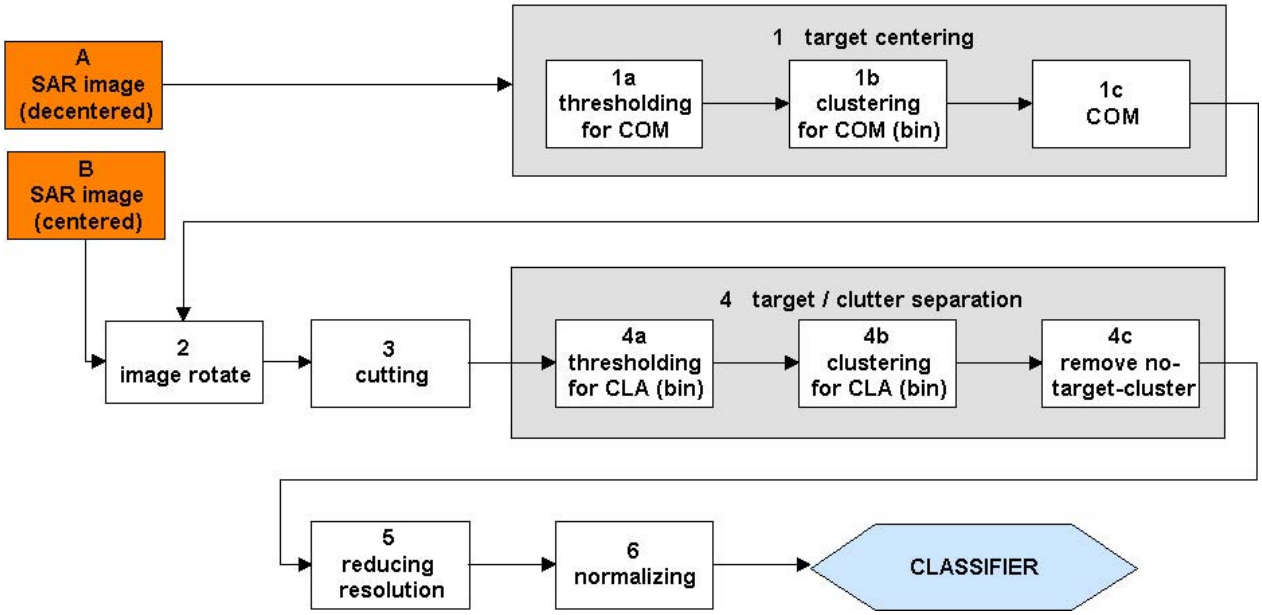

Figure 3: Data Preprocessing scheme (COM=Center of MASS; CLA=Classifcation)

Starting from the original datasets we have on the one side the centered MSTAR images (B) and the uncentered QinetiQ images (A). The image sizes are 128px x 128px for the MSTAR and 150px x 100px for the QinetiQ data. Because we use for our classification a pixelbased minimum distance Nearest Neighbour classifier (section 5.1) we have to center the data as accurately as possible.

To illustrate the preprocessing steps (fig. 4) we take an uncentered image of the QinetiQ data (fig. 2). The first step is to center the image. This can be done in three steps: first we determine a threshold to detect the target (step 1a). This threshold is adjusted on the image dimensions and the estimated ratio of target to background area. In our calculations we have used a 95%-median on the amplitude data, so that the 5% highest amplitudes are selected for further processing. In a second step we remove single pixels and clusters, which have less than 8 connected pixels. From the remaining large clusters we choose the largest one and replace the amplitudes with ones (step 1b, clipping) to eliminate the amplitude variations on the target. On this binary image we calculate the Center of mass "COM" (step 1c) with the indices i_m and j_m, where i and j are the pixel indices in range (R) and crossrange (CR) respectively and x are the amplitudes of the image data.

$$COM = (i_m, j_m) \,|\, i_m = \frac{\sum_{j=1}^{CR}\sum_{i=1}^{R} i \cdot x_{ij}}{\sum_{j=1}^{CR}\sum_{i=1}^{R} x_{ij}}; j_m = \frac{\sum_{i=1}^{R}\sum_{j=1}^{CR} j \cdot x_{ij}}{\sum_{j=1}^{CR}\sum_{i=1}^{R} x_{ij}}$$

At last the image with the original amplitudes is shifted according to the COM and the centering process is finished.

Step 2 is optional. If the azimuth orientations of the targets with respect to the sensor are known (ground truth or tracking information), they can be used to rotate the images so that all targets point in the same direction. Because of the different direction of rotation in both datasets the MSTAR images have to be rotated clockwise and the QinetiQ images counter clockwise. If no information about the aspect angle is

available, we ignore this step and proceed with step 3. Here a "cutting" step is introduced with a resulting concentration on the (centered) target. In our processing the clipped image has the dimension of 64px x 64px in both datasets.

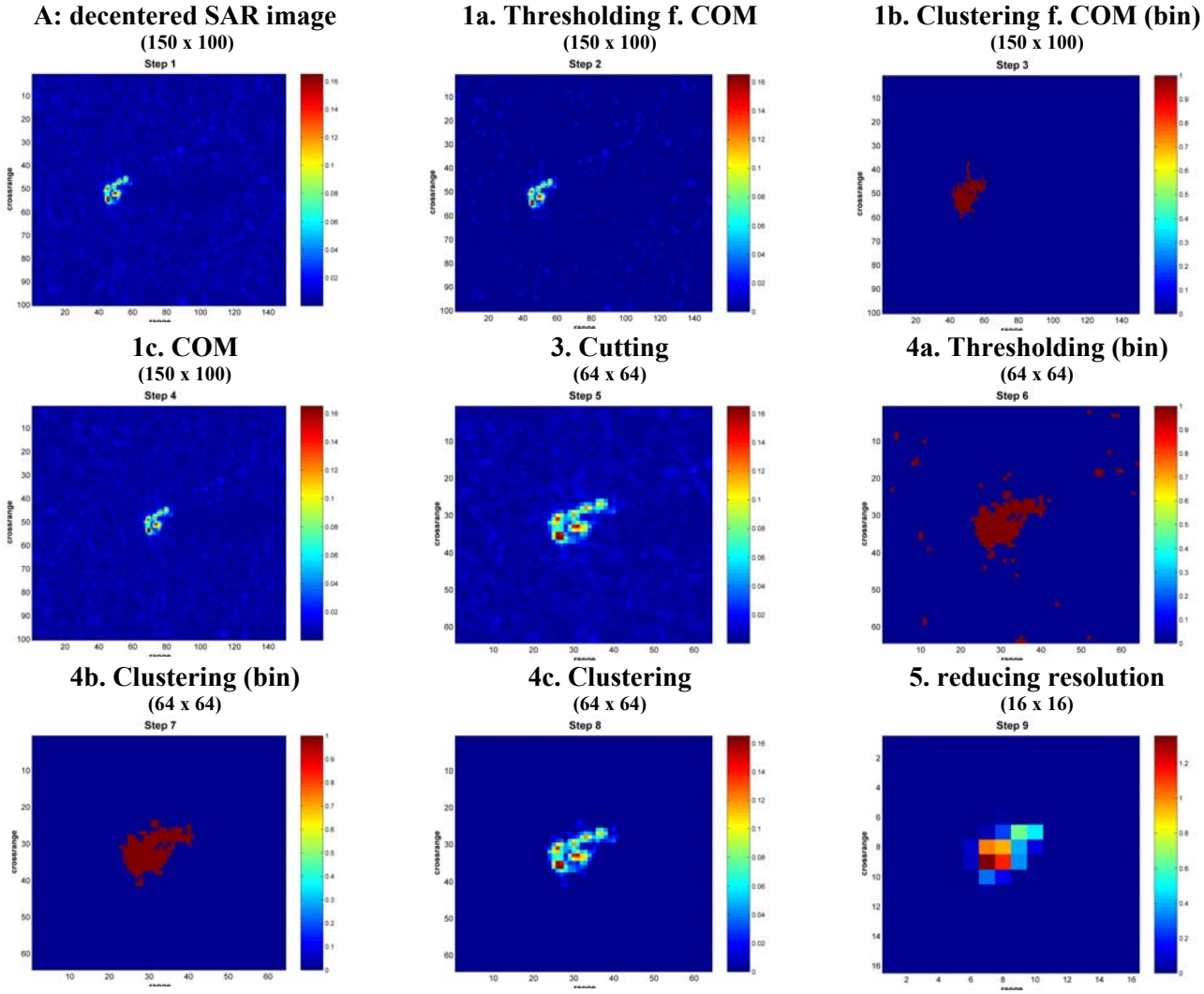

Figure 4: example for image processing before classification

In the fourth step we have the option doing image segmentation. This can be done in different ways: the normal way is to separate the target from the background clutter. Beside this we investigate cases of separating target shadow from image and clutter separately so that we can determine the influences of these parts of the image on the classification rate. In Fig. 4 the usual target segmentation is shown. Comparable to the COM calculation the thresholding (step 4a) and clustering (step 4b) of the image is done. The threshold T is adapted from a clutter level defined by a box around the target with $T=C_{mean}+3*C_{std}$ from the mean C_{mean} and standard deviation C_{std} of the clutter. After that connected pixels above this threshold are clustered, whereas little clusters and single pixels are removed. Additional clusters which are far away from the largest target cluster are eliminated (step 4c).

Step 5 of the preprocessing allows data reduction by reducing the image resolution. The clipped 64px x 64px image can be smoothed by a factor 2 or 4 so that the input image for the classifier has a size of 32px x 32px or 16px x 16px respectively.

To achieve a comparable set of preprocessed images the image is normalized to the image power of the preprocessed image finally (Step 6).

4.0 CLASSIFIER

For our investigations we used a simple pixel based Nearest Neighbor Classifier, which calculates the minimum distance between the amplitudes x of the test and the training images.

$$C(TE) = C(TR,\Delta) \mid \Delta(TE,TR) = \min\left\{\sum_{i=1}^{R}\sum_{j=1}^{CR}\left(x_{ij}^{TE} - x_{ij}^{TR}\right)^2\right\}$$

This means that all test images TE are compared with all replica images TR and the class of the test image C(TE) with the minimal distance Δ(TE,TR) to the replica TR is assigned. This minimum distance is equivalent to the correlation coefficient between the two images. The advantage of using a Nearest Neighbor classifier is on the one hand the simplicity of such a classifier (no parameters) on the other hand the missing training phase combined with its versatility of changing combinations of exspected targets. So this kind of classifiers is very simple and easy to use. Its drawback can be found in the bigger database and a somewhat longer decision time.

In the following section we applied this classifier on three different identification problems: a 5-class MSTAR, 10-class MSTAR and 9-class QinetiQ problem. Usually all test data are tested against all reference data (replica). A rejection class was not installed. The complexity of the three identification problems (number of test images and replicas, target classes) can be extracted from table 3.

To evaluate our results we compare the classification rates achieved with the NN-Classifier with other classifiers (linear and polynomial SVM, RBF).

5.0 CLASSIFICATION RESULTS

For our investigations we used three kinds of problems: 5-class MSTAR (M5), 10-class MSTAR (M10) and a 9-class QinetiQ (Q9) problem. We used forced decision classifiers with no rejection class. The test data is tested against all replicas.In our investigations we quantify the influence of the following key aspects on the classification rate:

- Target centering (using COM algorithms)
- Image segmentation (target, clutter, shadow)
- NN compared to different types of SVM classifiers
- Image resolution
- Target orientation (knowledge of the aspect angle)

Depending on computer power restrictions we sometimes worked with a reduced dataset. Especially for extensive calculations (decentering and shifting) we used the M5 instead of M10 dataset.

5.1 Target centering

Because we applied in our studies a pixel based classifier it is very important to adjust the image by target centering. This is indispensable when using the uncentered QinetiQ dataset, in contrast to this the original MSTAR dataset is centered already. Generally it cannot be assumed that the target images are centered in

a consistent format. To demonstrate the effect of classifying decentered and centered data we use the 5-class MSTAR (M5) dataset. First we make a random decentering of the target by ±10 pixel (V001), after that we decrease the misalignment to ±5 pixel (V002) and then we use our COM-algorithm to center the target (V003). When we finally allow additional shifts of ±1 pixel around the COM (V004), we get classification rates (97.9%) comparable to those of the original MSTAR centered data (V005, 98.1%). The results for these different centering studies are shown in table 4. Additional to our NN classifier the results of other classifier are demontrated (linear, polynominal, and RBF SVMs). The confusion matrices of the M5 (V004) and additionally of M10 and Q9 are given in fig. 5.

Table 4: Classification rates CLR [%] for centering studies V001-V005 with M5, 32px x 32px images with NN classifier (left table) and different types of SVM classifiers (right)

No	Case	CLR [%]
V001	±10 pix	**62.5**
V002	±5 pix	**80.2**
V003	±10 / COM	**96.1**
V004	±10 / COM / shift 1	**97.9**
V005	Original MSTAR	**98.1**

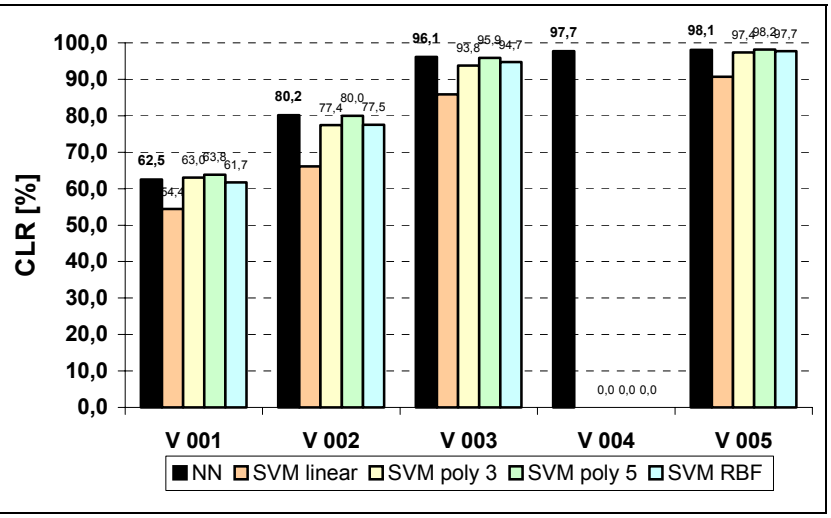

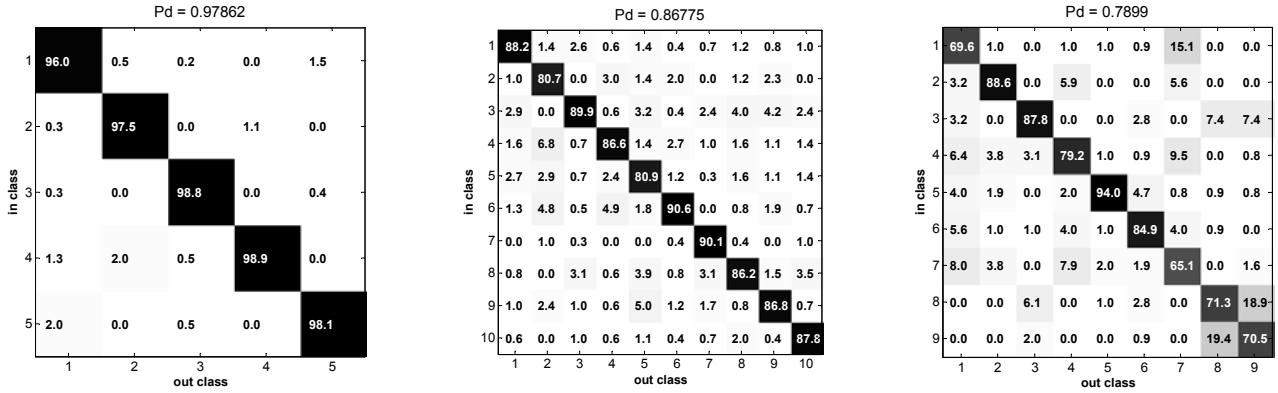

Figure 5: confusion matrices for SAR images of M5 (V004), M10 and Q9, 32px x 32 px

By applying this COM-centering algorithm on the 10-class MSTAR (M10) and 9-class QinetiQ (Q9) dataset (± 0 shifts) we get classification rates from 86.8% and 79.0% respectively (fig. 5).

5.2 Image segmentation

In section 5.1 we have calculated the classification rate of the *complete* SAR images by neglecting the influence of the clutter and the target shadow on the classification rate. In a next step we quantify this effect by separating and segmenting different parts of the image. So we are able to compute the real target

classification rate and analyze the influence of the surrounding clutter and target shadow. Fig. 6 shows different analyzed cases of segmented images, which were used as inputs for the NN-classifier. While the original image has a classification arte CLR of 97.9% the separated target classification rate drops down to 93.6%. Thus the target shadow and the clutter contribute to the classification of the SAR image. Quantifying this we get the CLR of the separated target shadow of 58.8% and a classification rate of the clutter of 99.4%. The evidence is that the clutter of the test and training images is highly correlated. To analyze this effect in detail, we put a defined zerobox over all targets and calculate the dependence of the clutter classification rate on the dimension of the box (which is a measure for the image clutter content ICC, fig. 7).

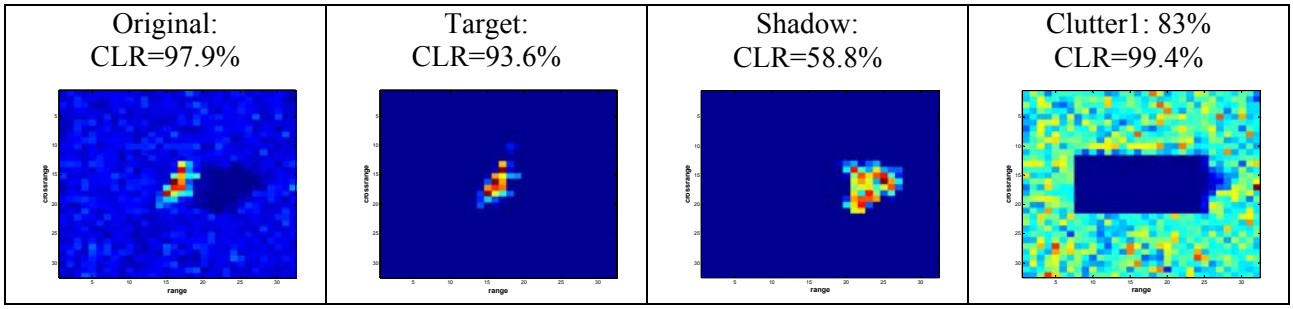

Figure 6: Segmentation of images for the M5 case; original, only target, only shadow, only clutter (from left to right)

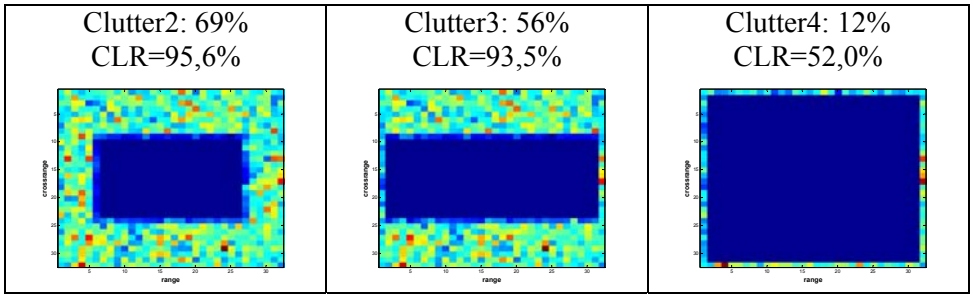

Figure 7: Clutter Classification rates CLR [%] for different image clutter content (ICC) for M5

The results are shown in fig. 8. Here we see the dependence of the clutter classification rate on the image clutter content for the two datasets M5 and Q9 classified with the NN-classifier and with a SVM-RBF classifier. In general the course of each case (M5 and Q9) is typical for the dataset, so the M5 lines are slightly convex curved, whereas the Q9 lines are more linear. The classification rate calculated with the NN classifier is much higher compared to the SVM-RBF classifier for the M5 case (up to 40%) and less high for Q9 case (4-10%). In all cases we get a significant classification rate only due to the clutter and the pixelbased minimum distance NN classifier seems to be more sensitive than the SVM classifier. This fact underlies a requirement on the used test and training dataset: To become independent from the clutter the targets in the test dataset have to be measured in different clutter environments than the training data.

To avoid this difficulty we separate the target from the clutter (step 4 in fig.3) resulting in a target classification rate of 82.7% for the M10 and 70.9% for Q9. The confusion matrices are shown in fig. 9.

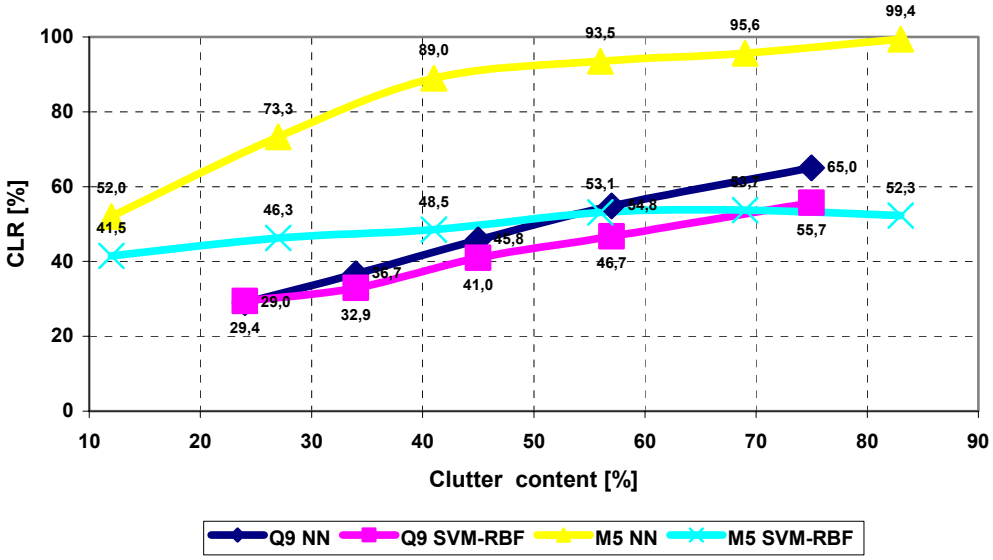

Figure 8: Classification rate CLR [%] of clutter for M5 and Q9 dataset dependent on the image clutter content

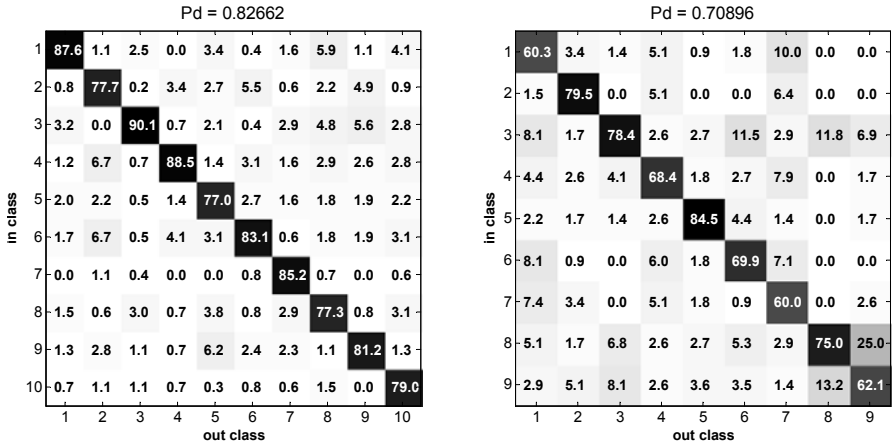

Figure 9: Confusion Matrix for M10 (l.) and Q9 (r.) for centered targets (without clutter)

This result can be optimized by shifting the COM-centered image by some pixels to compensate possible variations in the COM-calculations. A maximal target classification rate of 77.5% can be reached with an additional shift of ±4 pixels for the Q9 case (fig. 10). This fact points to the problem of the uncertainty in calculating the COM. The COM centering is only a coarse method, the fine adjustment has to be done in an additional step, for example with possible little shifts as applied here.

5.3 Classifier, image resolution and azimuth angle

Finally we compared exemplarily the identification results from the NN-classifier with different types of SVM-classifiers (linear, polynomial and RBF kernels). For these investigations (see fig. 11) we used the Matlab OSU Support Vector Machine Toolbox V.3 [4]. Because we know in both datasets the azimuth orientation of the target it is useful to rotate the images, so that all targets point in the same direction (step 2 in fig.3).

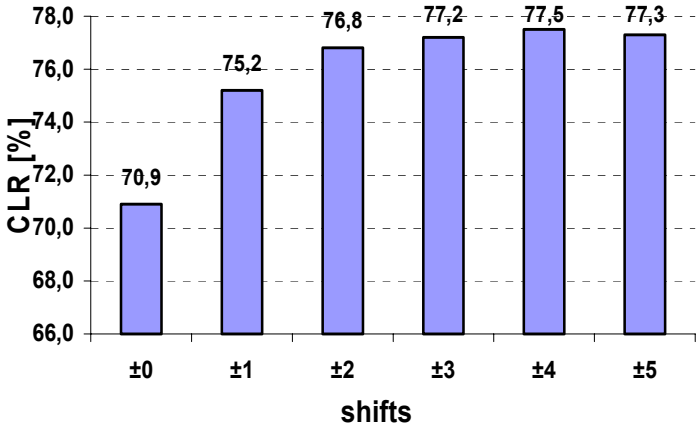

Figure 10: Classification rate for Q9 (NN, 32x32) with additional shifts on COM-centered targets

With this option the classification rates can be increased in all cases (4%-10%). The differences in the classification rate between the classifiers are marginal except the SVM with linear kernel, which produces 15-20% lower classification rates. In the M10 case we get maximal classification rates of 85-90%, in the Q9 case approximately 75%-82%. Additionally in fig. 11 the dependence of the image resolution (16, 32 and 64 pixel) is shown. In nearly all cases the best rates can be achieved using the 32 pixel (corresponding to 2ft (MSTAR) and 60cm (QinetiQ) resolution). So we cannot support the (often heard) statement that the highest resolution gets the best identification results.

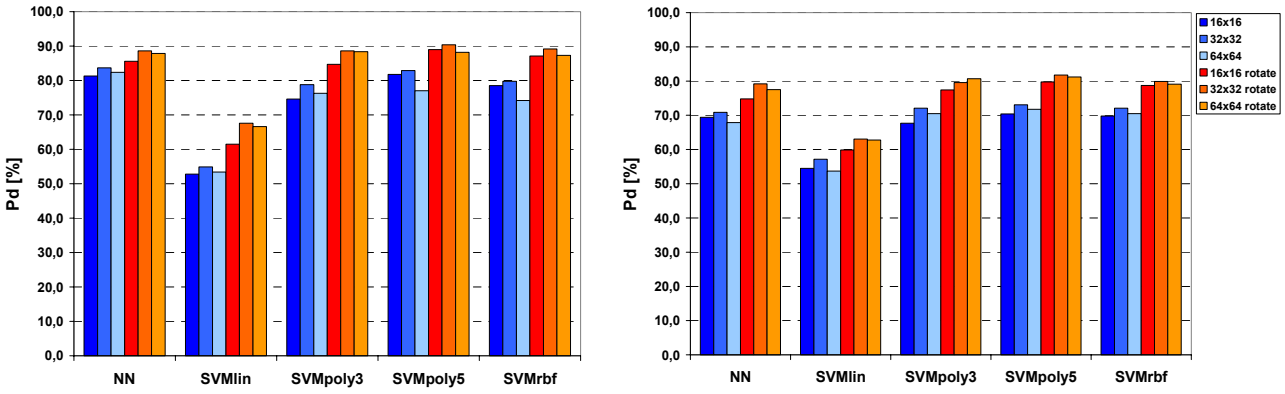

Figure 11: Classification rate [%] for different classifiers and different image resolutions (blue: without azimuth rotation, red: same azimuth orientation) for the M10 (l.) and Q9 (r.) case

6.0 CONCLUSION

Recapitulating we can conclude with the following results:

- Because of reasons of simplicity and the variety of parameters in other classifiers we used in our investigations in general a simple NN-classifier. Because our "features" are the image pixels target centering is essential. With a Center of Mass algorithm this can be done in a coarse way. Here we get target classification rates of 96.1% for the M5 case. Allowing additional shifts for a fine adjustment the classification rate can be increased to 97.9%.

- The clutter around the target and the target shadow has non negligible influence on the target classification rate. Of course the target must be separated from the clutter. This statement is true in general to reduce the S/C ratio as far as possilble. Doing this with the data under consideration in this report the classification rates drop from 87.3% to 82.7 (M10) and from 78.2% to 70.9% (Q9). With allowing shifts for fine adjustment classification rates of 77.5% can be reached for Q9. This surprising result can be explained by the "non-independence" between the test and replica images and underlies again the requirement for statistical independence of test and training data.
- For the M5 case the separated target shadow alone leads to a classification rate of 58.8%. Using only the clutter area of the images after removal of the target and shadow still classification rates varying from 52% to 99% (depending on the image clutter content ICC) were achieved, again highlightning the pronounced clutter correlation between test and training data. For clarification the dependence of the image clutter area on the classification rate was analyzed. For the Q9 case the clutter classifies the targets with 29%-65% depending on the ICC.
- By comparing the NN classifier with other classifiers (SVMs with different kernels) we get comparable results in the target classification rate.
- Dependent on the dataset best results can be reached with an image resolution of 32 pixels which correspond to 2ft (MSTAR) and 60cm (QinetiQ) pixel resolution.
- The classification rate can be tuned knowing the aspect angle of the target. Then the images can be oriented in the same direction, which increases the classification rate.

All these investigations show that the preprocessing of the data has extreme significance in the identification process. The applied classifier is then the last step with less importance. The requirements on the datasets are the strict independence of the measured test and training data.

ACKNOWLEDGEMENTS

We thank QinetiQ (UK) for providing the 9-class-dataset to the SET-053 group.

REFERENCES

[1] Moving and Stationary Target Acquisition Recognition (MSTAR), Program Review, Denver, CO, Nov. 1996

[2] Keydel, E.R., S.W. Lee and J.T. Moore: MSTAR Extended Operating Conditions. A Tutorial, In Proc. Of SPIE, Vol. 2757, Algorithms for Synthetic Aperture Radar Imagery III, p.228-242, 1996

[3] Ross, T.D. and J. Mossing: MSTAR Evaluation Methodology. In Proc. of SPIE, Vol. 3721, Algorithms for SAR Imagery VI, p.705, Orlando, USA, 1999

[4] Junshui Ma, Yi Zao: OSU Support Vector Machines Toolbox V3.00 for Matlab, Feb. 2002

[5] Gelf, S., J. Schiller and J. Chadwick: Non-Cooperative Air Target Identification using radar range profiles, 5th International Military Sensing Symposium, Gaithersburg, MD, 2002

[6] Rosenbach, K. and J. Schiller: Non-Cooperative Air Target Identification using radar imagery, IEEE International Radar Conference – RADAR 2000, Alexandria, VA, 2000